AMEGHINIANA
A GONDWANAN PALEONTOLOGICAL JOURNAL

Submitted: October 28th, 2020 – **Accepted**: July 23th, 2021 – **Posted online**: July 31th, 2021

To link and cite this article:

doi: 10.5710/AMGH.23.07.2021.3412

BIOMECHANICAL SKULL STUDY OF THE AETOSAUR *NEOAETOSAUROIDES ENGAEUS* USING FINITE ELEMENT ANALYSIS

JEREMÍAS R. A. TABORDA[1,2], JULIA B. DESOJO [1,3], AND EDUARDO N. DVORKIN[4]

[1] Consejo Nacional de Investigaciones Científicas y Técnicas (CONICET)

[2] Centro de Investigaciones en Ciencias de la Tierra (CICTERRA), Universidad Nacional de Córdoba, CONICET, FCEFyN, Vélez Sarsfield 1611, Ciudad Universitaria (X5016GCA), Córdoba, Argentina.

[3] CONICET-División Paleontología Vertebrados, Museo de La Plata, Paseo del Bosque s/n°, B1900FWA La Plata, Argentina. (*julideso@fcnym.unlp.edu.arm*)

[4] SIM&TEC, Av. Pueyrredón 2130 5to "A", C1119ACR, Buenos Aires, Argentina. (*edvorkin@simytec.com*)

31 pag. (text + references); 07 figs.; 04 tables

Running Header: TABORDA *ET AL*: FEA OF AN AETOSAUR SKULL

Short Description: Computational biomechanics of the aetosaur *Neoaetosauroides engaeus* helps clarify its feeding ecology.

Corresponding author: Jeremías R. A. Taborda (*jeremias.taborda@gmail.com*)

Abstract Aetosaurs are quadrupedal archosaurs that had a worldwide distribution during the Late Triassic. They had small heads relative to their body size and a long tail, and they are characterized by a dorsal and ventral carapace formed by ornamented and articulated osteoderms. Although aetosaurs historically have been considered the only herbivorous early pseudosuchian archosaurs, few analyses quantitatively assess their feeding habits, and some authors have proposed omnivorous and/or scavenging habits for the group. *Neoaetosauroides engaeus* Bonaparte, 1969 is an aetosaur from Late Triassic of the Los Colorados Formation, La Rioja, Argentina. *N. engaeus* is known from three relatively well preserved skulls, making it an excellent taxon to study the feeding ecology. We applied the Finite Element Method (**FEM**) to estimate bite force and to evaluate the structural response of the skull at different positions during food processing. Our results show that the skull of *N. engaeus* generated a bite force of 3.6 kN, a magnitude comparable with the measurement made in *Alligator mississippiensis*, and could resist lateral and longitudinal forces during feeding. This indicates that *N. engaeus* was capable of hunting of small living prey (*e.g.*, cynodonts) with its jaws, and/or dragging carcasses of larger sizes (*e.g.*, dicynodonts). These results support possible zoophagy or omnivory for *N. engaeus*, thus expanding the potential ecological roles of aetosaurs.

Keywords. Pseudosuchia. Biomechanics. Feeding habits. Finite Element Model. Bite force estimation.

Resumen. ESTUDIO BIOMECÁNICO DEL CRÁNEO DE UN AETOSAURIO (*NEOAETOSAUROIDES ENGAEUS*) USANDO ANALISIS DE ELEMENTOS FINITOS. Los aetosaurios son un grupo de arcosaurios con distribución mundial durante el Triásico Tardío. Tenían cabeza pequeña en relacionada al tamaño del cuerpo y una cola larga, y se

caracterizan por tener una armadura dorsal y ventral, formada por osteodermos ornamentados y articulados. A pesar de que los aetosaurios se consideraron históricamente como los únicos herbívoros entre los primeros arcosaurios pseudosuquios, pocos análisis evalúan cuantitativamente sus hábitos de alimentación, y algunos autores han propuesto hábitos omnívoros y/o carroñeros para este grupo. *Neoaetosauroides engaeus* Bonaparte, 1969, es un aetosaurio de Triásico Tardío de la Formación Los Colorados, La Rioja, Argentina. Se conocen tres cráneos relativamente bien conservados de *N. engaeus*, siendo un excelente taxon para realizar estudios de la ecología de alimentación. Aplicamos el Método de los Elementos Finitos (MEF) para estimar la fuerza de mordida y evaluamos la respuesta estructural del cráneo en diferentes situaciones durante la alimentación. Nuestros resultados muestran que el cráneo de *N. engaeus* generó una fuerza de mordida de 3.6 kN una magnitud comparable con mediciones realizadas en *Alligator mississippiensis*, y podría resistir esfuerzos externos laterales y longitudinales. Esto indicaría que *N. engaeus* podría capturar presas vivas de pequeño tamaño (*e.g.*, cinodontes) con sus mandíbulas, y/o arrastrar cadáveres de mayor tamaño (*e.g.*, dicinodontes). Estos resultados brindan una nueva evidencia para respaldar la posible zoofagia u omnivoría para *N. engaeus*, ampliando los roles ecológicos de los aetosaurios previamente conocidos.

Palabras clave. Pseudosuchia. Biomecánica. Hábitos alimentarios. Modelo de elementos finitos. Estimación de la fuerza de mordida.

AETOSAURS ARE A GROUP OF PSEUDOSUCHIAN ARCHOSAURS from the Late Triassic with a near cosmopolitan distribution; their fossils have been found in the Americas, Africa, Europe, and India (Heckert & Lucas, 2002; Desojo *et al.*, 2012, 2013). Body size of aetosaurs ranges from small species like *Aetosauroides ferratus* Fraas, 1877 (body length ca. 1 m) to larger species such as *Desmatosuchus spurensis* Case, 1920 (body length ca. 6 m) (Sawin, 1947; Walker, 1961; Desojo, 2003; Desojo & Báez, 2005; Schoch, 2007; Parker, 2008; Heckert *et al.*, 2010; Desojo *et al.*, 2013; Small & Martz, 2013; Taborda *et al.*, 2013).

Aetosaurs were quadrupedal armored animals, with a semi-erect posture (Parrish, 1986; Desojo & Báez, 2005; Padian *et al.*, 2010). They have a relatively small head that is approximately 12% of the total length of the body (Taborda, 2011). Aetosaurs are characterized by ornamented osteoderms covering almost the entire body (*e.g.*, Casamiquela, 1961; Walker, 1961; Long & Ballet, 1985; Parker, 2007, 2008; Schoch, 2007; Heckert *et al.*, 2010; Cerda & Desojo, 2011; Taborda, 2011; Desojo *et al.*, 2013; Small & Martz, 2013). The osteoderms are the most common aetosaur skeletal element preserved, but many taxa are known from partial or complete skulls (*e.g.*, *Aetosaurus*, *Desmatosuchus*, *Typothorax*, *Neoaetosauroides*, *Aetosauroides*, *Stenomyti*, *Stagonolepis*, *Scutarx*; Bonaparte, 1969, 1971; Heckert & Lucas, 1999; Small, 2002; Schoch, 2007; Sulej, 2010; Desojo & Ezcurra, 2011; Small & Martz, 2013; Desojo *et al.*, 2013; Parker, 2016, 2018a, 2018b; Biacchi Brust *et al.*, 2018).

The skull of aetosaurs is triangular in dorsal and lateral views. In most taxa, the snout is long and anteriorly pointed, with the anterior end of premaxilla laterally expanded, but it tapers continuously towards the tip (unexpanded) in *Aetosaurus ferratus*, *Stenomyti huangae*, and *Paratypothorax andressorum* (Gregory, 1953; Schoch, 2007; Small & Martz,

2013; Schoch & Desojo, 2016; Parker, 2018b). In all taxa except *Aetosauroides scagliai*, the lower jaw is anteroposteriorly elongate, slender, and characteristically 'slipper-shaped' (Casamiquela, 1961; Desojo & Ezcurra, 2011; Desojo *et al.*, 2013). The anterior portion of the dentary is toothless and lacks evidence of keratinous beak (Parrish, 1994; Desojo & Vizcaíno, 2009; Desojo *et al.*, 2013).

Aetosaur tooth implantation is thecodont in the premaxilla and dentary, and it is sub-thecodont in the maxilla (Taborda & Desojo, 2010). In general, tooth crowns are either bulbous or laterally compressed, with a constriction at the base separating the crown from the cylindrical root and a slightly recurved conical tip (Walker, 1961; Schoch, 2007; Taborda & Desojo, 2010; Desojo *et al.*, 2013). The surface of tooth crowns is ornamented by a longitudinal furrow in some taxa (*e.g.*, *Neoaetosauroides engaeus*, *Stagonolepis olenkae*, *Aetosaurus ferratus*), and a carina with denticles in others (*e.g.*, *Aetosauroides scagliai*, *Stagonolepis olenkaen*). Wear facets are present in some taxa (*i.e.*, *Aetosauroides scagliai*, *Stagonolepis olenkaen*, *Desmatosuchus smalli*, *Desmatosuchus haplocerus*, *Stagonolepis robertsoni*; Small, 2002; Parker, 2005; Sulej, 2010; Taborda & Desojo, 2010; Desojo *et al.*, 2013; Taborda, 2016; Biacchi Brust *et al.*, 2018).

Historically, aetosaurs were the only Triassic pseudosuchian group hypothesized to be herbivorous (*e.g.*, Walker 1961; Parrish 1994), an inference based northern hemisphere taxa such as *Stagonolepis robertsoni*, *Typothorax coccinarum*, and *Longosuchus meadei*. However, some authors proposed that *N. engaeus*, from the southern hemisphere, was zoophagous or omnivorous, based on morphological and functional analyses (*e.g.*, Bonaparte, 1973, 1978; Small, 2002; Desojo & Vizcaíno, 2009; Taborda, 2016).

Among South American aetosaurs, *N. engaeus* has the best record of skull material; three partial skulls are known and one mandible is almost complete, making it an excellent

112 taxon to investigate feeding ecology and further understand the ecological roles of
113 aetosaurs. Unfortunately, among living archosaurs (crocodylians and birds) there are no
114 analogous forms similar to aetosaurs; thus, it is difficult to find an equivalent ecological
115 role. For this reason, it is necessary to use reconstructed models and methods (*e.g.*,
116 engineering software) to evaluate biomechanical properties and performance of extinct
117 animals and estimate their ecological roles.

118 The first functional analysis on an aetosaur was on *N. engaeus* using a geometric method
119 (Desojo & Vizcaíno, 2009). In this study, the authors estimated the moment arm of the
120 mandibular adductor muscles of *N. engaeus* and using this information estimated the bite
121 performance of other aetosaurs (*S. robertsoni* and *Desmatosuchus*) and compared them
122 with the living pseudosuchian *Alligator mississippiensis*. The authors concluded that the
123 cranio-mandibular design of *N. engaeus* optimized the bite force over the closing velocity.
124 Based on this conclusion, these authors suggested a zoophagous diet for this taxon, contrary
125 to the herbivorous hypothesis proposed previously for all the taxa known for this clade.

126 Finite element method (**FEM**) is an excellent tool for evaluating the mechanical
127 properties of a skull. This engineering method allows different loads to be applied in a
128 model of 3D structure and evaluates the structural response (Zienkiewicz & Taylor, 1994a,
129 1994b; Bathe, 1996). In biological and paleontological studies, finite element analysis
130 (**FEA**) is used to evaluate mechanical properties and analyze biomechanical hypotheses
131 concerning the ecological role of organisms (*e.g.*, Richmond *et al.*, 2005; Ross, 2005;
132 Rayfield, 2007; Wroe *et al.*, 2007; Moreno *et al.*, 2008; Degrange *et al.*, 2010; Porro *et al.*,
133 2011; Curtis *et al.*, 2011; Young *et al.*, 2012; Fortuny *et al.*, 2012, 2016; Lautenschlager *et*
134 *al.*, 2013; Schwager *et al.*, 2013; Button *et al.*, 2014, 2016; Snively *et al.*, 2015; Taborda &
135 Desojo, 2015; Cox *et al.*, 2015; Lemanis *et al.*, 2016 and references therein; Dynowski *et*

al., 2016; Sellers *et al.*, 2017; Lautenschlager, 2017; Cost *et al.*, 2020). In order to understand the ecological role of *N. engaeus*, we tested the mechanical response of its skull using FEA under different scenarios of food apprehension.

MATERIAL AND METHODS

Institutional abbreviations

PULR: Paleontología Museo de Ciencias Naturales, Universidad Nacional de La Rioja, La Rioja, Argentina.

PVL: Paleontología de Vertebrados, Instituto Miguel Lillo, Tucumán, Argentina.

ZPAL: Institute of Paleobiology, Polish Academy of Sciences, Warsaw.

Material

Three skulls referred to *N. engaeus* were studied: PVL4363, PVL5698, and PULR108. The holotype was excluded, because only the lower jaws and postcranial skeleton are preserved. The three referred skulls of *N. engaeus* are incomplete, but together they were sufficiently complete to reconstruct the skull (Fig. 1). The complete model was used to perform the analysis (Lautenschlager, 2016; Taborda, 2016).

Skulls of *N. engaeus* were scanned using Computer Tomographic (**CT**) acquisition methods. The CT data were acquired on a medical axial tomography multi-slicer of 64-channel in the Clínica la Sagrada Familia (Buenos Aires, Argentina). The DICOM file specifications and associated data obtained for each specimen are detailed in Table 1 (see Supplementary Information for preview video of the CT scan). For segmentation and 3D model generation, we used the software 3D Slicer v4.1.1 (Fedorov et al., 2012). We aligned and merged all 3D models obtained by segmentation using CAD software (Meshmixer

v3.4.35; Geomagic Wrap v2017.0.0.111; Rhinoceros 3D v5) to reconstruct the complete skull and mandible of *N. engaeus* (Fig. 1). These 3D models are the basis for the biomechanical analysis of the present contribution.

3D skull reconstruction

PVL5698 has the best three-dimensional (**3D**) preservation, therefore we use it as a base for the complete skull model. Through segmentation, we extracted the sediment that occupied the internal cranial cavities and recovered most of the bones (Fig. 1.1). Unfortunately, this specimen does not preserve the snout, mandible, or the edges of temporal fenestrae, which were lost by aggressive mechanical preparation. For this reason, we reconstructed these regions based on PVL4363 and PULR108. The CT scan of PVL5698 is available in von Baczko *et al.* (2018).

PVL4363 preserves some palatal bones and part of the mandible. Unfortunately, most of the skull is preserved as an internal cast (von Baczko *et al.*, 2018). For this reason, the missing bones were generated as a virtual cast from the surface of the fossil. We obtained the general morphology of the snout, the margin of the temporal fenestra and orbit, and the mandible (Fig. 1.2).

PULR108 preserves the molds of the teeth and the labial surface of the maxilla. These allowed us to generate these structures by a virtual cast (Fig. 1.3) and finish the complete skull model for analysis.

Tooth reconstruction and interpretation

The herbivorous habit of aetosaurs was mainly inferred from tooth morphology of Laurasian specimens such as *Desmatosuchus*, which shows large wear surfaces (Walker, 1961; Parrish, 1994; Heckert & Lucas, 2000; Small, 2002; Desojo *et al.*, 2013). However, aetosaurs have a number of tooth morphotypes, likely related with differences feeding

habits and phylogeny. For this reason, it is essential to reconstruct and analyze the tooth morphology in *N. engaeus* in conjunction with the rest of the skull.

The available teeth of *N. engaeus* are poorly preserved or have been abraded through aggressive preparation. Their original morphology is known principally by one cast of the upper jaw of PULR108, which is the source for the dental morphology in our reconstruction.

Neoaetosauroides engaeus has four teeth in the premaxilla and eight in the maxilla and dentary. All teeth have the same morphology, but their size varies among the premaxilla, maxilla, and dentary (Desojo & Báez, 2007) (Fig. 2.1-2.2). The teeth of *N. engaeus* have a bulbous crown with a little labiolingual compression, a conical apex slightly curved distally, and a concave lingual surface (Fig 2.3). A small neck separates the sub-cylindrical root from the base of the crown (Fig 2.3). The roots are approximately twice the length of the crowns. This morphology is similar to that of the distal teeth of the living crocodylians *Caiman yacare* (Fig. 2.4) and *C. latirostris* (Daudin, 1802). The crown surface is ornamented with axial grooves in *N. engaeus* (Fig. 2.3), resembling the condition reported in *Stagonolepis olenkae* (Fig. 2.5; Sulej, 2010).

It is probable that the tooth crowns had carinae with denticles like as those of *S. olenkae* or *A. scagliai* (Sulej, 2010; Desojo *et al.*, 2013; Biacchi Brust *et al.*, 2018). Although the preservation of *N. engaeus* teeth does not allow us to confirm the presence of denticles, we can confirm that *N. engaeus* teeth do not have wear facets, contrasting with those observed in other aetosaurs such as *Desmatosuchus* and *Stagonolepis robertsoni*.

The premaxillary and dentary teeth have typically thecodont implantation, but in the maxillary teeth the implantation is sub-thecodont (*sensu* Bertin *et al.* 2018), with interdental plates. The latter implantation is visible in PVL4363, which shows the

incomplete alveoli margin in the lingual face of maxillary. The same specimen preserves fragments of maxillary interdental plates, which were probably lost during the fossilization process. These would have completed the lingual margin of the alveoli (see 3D model in Supplementary Information). This condition is common in aetosaurs, and it is recorded in most of the species, including *Longosuchus meadei*, *Desmatosuchus* , *Calyptosuchus wellesi*, *Stagonolepis robertsoni*, and *S. olenkae* (Taborda & Desojo, 2010; Parker, 2018a).

Cranio-mandibular joint

During the bite in vertebrates, the configuration of the adductor chamber muscles can generate movements in the cranio-mandibular joint that are not strictly rotational (Taborda, 2016). To allow these non-rotational movements without losing joint support, we used a 3D structure that surrounded the cranio-mandibular articulation area (see Supplementary Material). This 3D structure simulates the soft tissue associated with the joint that permits the independent movements of the cranium and mandible.

Adductor chamber reconstruction

Because bite forces are produced by adductor muscles in living tetrapods (Kardong, 2011), accurate 3D representation of musculature is important to create a realistic performance of the model (Gröning *et al.*, 2013). We reconstructed the 3D adductor chamber musculature using the CAD software Meshmixer v3.4.35 (Fig. 3).

The reconstruction of the adductor musculature in *N. engaeus* was principally based using the model of the living crocodylians *Caiman yacare*, *C. latirostris*, and *Alligator mississippiensis* and the squamates *Iguana iguana* and *Sphenodon* sp. (Iordansky, 2000; Holliday & Witmer, 2007; Jones *et al.*, 2009; Bona & Desojo, 2011; Holliday *et al.*, 2013; Taborda, 2016). Additionally, we performed muscle dissection of *C. yacare* and *I. iguana* (Taborda, 2016). Based of this information, we reconstructed the *musculus adductor*

mandibulae posterior (**mAMP**), *musculus adductor mandibulae externus superficialis/medialis/profundus* (**mAMEs/m/p**), *musculus pseudotemporalis* (**mPST**), *musculus intramandibularis* (**mIM**), and *musculus pterygoideus ventralis*/*dorsalis* (**mPTv/d**). We estimated the force of each muscle from their reconstructed cross-sectional area (Table 2).

The *transiliens* cartilage is an important element in the adductor chamber architecture of archosaurs because it is the nexus between mPsT and mIM that permits transfer of muscle force during the bite (Tsai & Holliday, 2011). The position of the *transiliens* cartilage is ambiguous in aetosaurs because it lacks a bone insertion. Walker (1961) positioned the *transiliens* cartilage in *Stagonolepis robertsoni* over the coronoid process of the surangular of the hemimandible. The same position for this cartilage is assumed for all aetosaurs (Desojo & Vizcaíno, 2009). *N. engaeus* lacks this process, and so we positioned the *transiliens* cartilage on the medial margin of the surangular, over the anterior margin of the mandibular fenestra. For the transiliens cartilage we using a fictitious material softer than bone to emulate the real structure (Table 3).

Finite element model

For the finite element model (**FEm**), we considered the *N. engaeus* skull to be a completely akinetic structure. The mesh of FEm is composed by tetrahedral elements with four nodes. For the bone structures, we assigned a single set of material properties (Table 2) obtained from *Alligator mississippiensis* (Zapata *et al.*, 2010). For the cranio-mandibular articular structure, we generated a semi-rigid fictitious material to emulate the tissue complex (see Supplementary Material 2) that mirrors living reptiles (Table 3).

The FEm model was fixed (restricted all degrees of freedom) at the articular surface of occipital condyle and attachment surface of neck muscles. The rest of the boundary

conditions are explained below for each analysis. We used the software FEMAP v10.3.1 to create the FEm and the software ADINA v8.7.3 to solve the system.

We did not compare our results from *N. engaeus* with those of other animals, because the structural responses resulting from the FEA analysis depend on the analyzed structure morphology (Zienkiewicz & Taylor, 1994b, 1994a; Bathe, 1996). For this reason, we use the modulus of 3.6GPa, for bones (Reid, 1996), as a reference of maximum tolerance to the material. Considering the safety factor concept (Gonzalez, 1974), we assume that biological structures they usually work far below the maximum resistance of materials to avoid being exposed to any injury (*e.g.*, fractures, cracks, etc.). In the interpretation of our results, we considered a stress normal condition to values around 1.8 GPa (*i.e.*, the middle of bone shear modulus: 3.6 GPa).

Muscle modeling

The muscular force is usually applied as a directed vector whose direction is estimated from the centroids of muscular attachment surfaces (*e.g.*, Ross *et al.*, 2005; Degrange *et al.*, 2010; Porro *et al.*, 2011; Marcé-Nogué *et al.*, 2015; Snively *et al.*, 2015). Here, we used a different method to incorporate the muscular action on the FEm. This method consists of the creation a system of contractile bars (attached of the bone surfaces) that mirror muscle morphology (*e.g.*, Wroe *et al.*, 2008, 2013; McCurry *et al.*, 2015; Attard *et al.*, 2016; Taborda, 2016). We named this system “muscular action bars” (**MAB**) (Taborda, 2016). MAB are cylindrical segments with controlled contraction capacity of theoretical material that simulate the action of real muscles (Supplementary Material 2). These MABs link the attached surfaces, in the skull and mandible, for each muscle (Fig. 4.1- 4.2). In this way, the muscle force is applied when these elements contract, in the bite model, simultaneously pulling the cranium and mandible.

We modeled *musculus pterygoideus ventralis* (mPTv) and *musculus pterygoideus dorsalis* (mPTd) as multi-line arrays for the insertion zones (resembling that used for the other muscles), and a polygonal line for the middle of body muscle.

RESULTS OF THE BIOMECHANICAL ANALYSIS

Bite force simulation

We considered the tetrapod cranio-mandibular complex to be a working system of two opposite class 3 levers (Borelli, 1680) in order to design a bite force estimate that is independent of measurements of other magnitudes of the body (*e.g.*, body mass, length of skull). In this system, the muscles of the adductor chamber pull from the mandible and the cranium in opposite directions from the point of articulation to apply the bite force to the food. Simple lever arm physics works for one-dimensional (**1D**) systems (*i.e.*, straight lever arms without thickness variable); but the cranio-mandibular system is a complex 3D structure. The cranio-mandibular system is composed by bones with curved lines in different directions, and for this reason applying simple lever arm physics to this complex system would be incorrect. The best approach to analyzing the cranio-mandibular complex performance is using continuum mechanics, for this reason, we apply the finite element method to measure the bite force.

Considering the action-reaction law (Lex. III, Newton, 1687), we can estimate the reaction force in a tooth during the bite. For this, we fixed some points in the model (Fig. 4.3) during the bite simulation and measured the reaction force at the same points. The total bite force is obtained by summing the modulus of all reaction forces at the fixed points (when the MABs contracts) in each case. We tested the accuracy of these measurements using the *Caiman yacare* model (Supplementary Material), in which the resulting bite force

was 3.2 kN, which is close to the result obtained using regressions from *in vivo* measurements (Supplementary Material). This method, which only depends on the cranio-mandibular morphology and muscular configuration, is an excellent tool to estimate the bite force in extinct groups that do not have extant representatives or analogs.

We measured the bite force at different points of the jaw of *N. engaeus* (Fig 4.3) under different feeding scenarios, such as unilateral (for the middle and posterior portion) and bilateral situation (for anterior portion of jaw).

The results obtained (Table 4) for the second maxillary tooth (3.6 kN) and the last maxillary tooth (5.5 kN) are higher than mean measurements in the most prominent caniniform and molariform teeth of the upper jaw (3.3 kN and 5.1 kN respectively) in the living crocodylian, *Alligator mississippiensis* (Erickson *et al.*, 2012; Sellers *et al.*, 2017). Sellers *et al* (2017) estimated an *in vivo* bite force of 3.4 kN for an *A. mississippiensis* (skull length = 33 cm). Based on our calculations, *N. engaeus* (skull length ca. 20 cm) probably had a more powerful bite.

The results of the model do not show areas with high stress values in the cranium or mandible. The stress values in all structures analyzed were very low compared with the material modulus. These results confirm that there are no areas of important kinesis in the skull at the time of the bite, otherwise, high stress areas would be seen where these kinesis zones should be.

In all bite tests, we observed that the stress in the cranium is concentrated in the posteriolateral region (quadrate, quadratojugal and jugal bones), principally over the cranio-mandibular joint area (Fig. 5). In the mandible, the stress is distributed in the middle area, principally over the angular and the surangular bones, always anterior of the cranio-mandibular joint, up to the point of contact with the food item. In the case of a unilateral

bite, an increase in stress was also observed in the symphyseal area, owing to the muscular force acting with different resistance on both hemimandibles. During the bite test done between the distal end of the dentary and the first premaxillary teeth, stress was distributed in the concave central area of the mandible. In this case, the mandible shape in this area behaves like an arch bridge, thus giving greater resistance and stability to the structure during the bite.

Skull reaction to external force in the jaw during the bite

In order to analyze the stress pattern during food intake/manipulation, we recorded the response of the skull and mandible for two situations of external force on different points in the jaw: lateral load force and tractive load force.

Lateral load force. This setting corresponds movement caused by live prey trying to escape. In this situation, the prey exerts a lateral force perpendicular to the sagittal plane of skull. This scenario was used to evaluate the ability of *N. engaeus* to capture live prey.

Tractive load force. The purpose of this scenario was to evaluate the scavenging ability of *N. engaeus*. During the dragging of a carcass, the forces over the skull are principally longitudinal, for this, the load forces are applying in longitudinal direction.

The load force was applied bilaterally and divided equally among all the points. In all tests, the load force was applied simultaneously with the bite simulation to mimic reality. In both load scenarios (lateral and tractive load force), we applied a force of 1 kN, the force equivalent to a static mass approximately of 102 kg. However, considering that animals in movement can generate accelerations of twice that of gravity (Halsey & White, 2010; Qasem *et al.*, 2012), this test can also correspond to capturing live prey of 51 kg, this is equivalent to the body mass of *N. engaeus* (50 kg) estimated by Taborda *et al*. (2013).

The results of different scenarios in the two external load situations show that the skull exhibited a maximum stress with a value close to the middle of the shear modulus of material in all tests (Fig. 6). This indicates that the structural integrity of the skull is not compromised under these load conditions.

Comparing the stress distribution for all tests in both scenarios (dismissing the stress by artifact in the load points), we observe that the skull structure is little more resistant to tractive forces than lateral forces. However, in all cases the stress is concentrated at the cranio-mandibular joint, this is an expected effect because the articular area is a zone of structural weakness.

During the lateral load force test, high stresses were concentrated over the posterior area of the cranium and mandible, similar to that observed in the bite test. In the cranium, the stress patterns show a greater participation of the supraoccipital and parietal areas, and to a lesser extent of the frontal zone. These patterns may result from the neck muscles stabilizing the head. In turn, during the tractive force test, the stress is concentrated mainly at the cranio-mandibular joint area, because the stabilization of mandible to prevent anteroposterior sliding is crucial in this type of load force.

Vertical force reaction

Some authors proposed that *N. engaeus* could have dug with the snout to search for food (Bonaparte, 1971; Desojo & Vizcaíno, 2009; Desojo *et al*., 2013). To simulate the strain generated during the digging by the snout, we applied the bilateral load force on vertical direction over the dorsal surface of the shovel-shape expansion of the premaxillae. We only tested the possibility of digging with the snout because other capacities such as digging with fore limb (Dróżdż, 2018) exceed the objectives of this work. We applied the load force of 100 N, equivalent to load a static mass approximately of 10 kg, over the dorsal surface of

premaxillary expansion, at an angle of 45º from vertical. The results of this analysis show high stress levels near the articulation between nasal and premaxilla, and in the palatine (Fig. 7). The values of stress are greater than the bone shear modulus on these affected areas, which indicates that the skull would be exposed to possible injuries (*e.g.*, fractures). This result implies that the narrow premaxilla-nasal articulation of *N. engaeus* would be poorly-suited for digging with the snout to search for food.

DISCUSSION and CONCLUSIONS

Our biomechanical analysis shows that the skull of *N. engaeus* was able to withstand both lateral and tractive force loads in the same way. These results suggest that the skull could resist the stress generated during hunting or carrion eating. In contrast, the vertical force load scenario, the stress level in the snout are greater than the shear modulus of bone. This leads to the conclusion that *N. engaeus* couldn't bear the effort of digging with your snout to food searching. Additionally, ee estimate that the bite force of *N. engaeus* was equivalent to measurements obtained for the living crocodylian *Alligator mississippiensis*. This new evidence supports the hypothesis of zoophagy for this taxon (Bonaparte, 1978; Desojo & Vizcaíno, 2009).

The absence of wear facets on the teeth of *N. engaeus* (Taborda & Desojo, 2010; Desojo *et al.*, 2013), suggests its diet did not include substantial abrasive material. The absence of these facets wear facts is not attributable to dental substitution, because we did not observe any replacement teeth by CT scan on any skull. In fact, *N. engaeus* has a low rate of dental replacement. Therefore, we interpret *N. engaeus* to have had a zoophagous diet (hunter or scavenger). We do not discard the possibility that *N. engaeus* also consumed herbaceous materials, but the tooth morphology of *N. engaeus* is not consistent with that of an obligate

herbivore. Comparing the morphological similarity between *N. engaeus* teeth with the posterior teeth of *C. yacare* or *C. latirostris*, and considering the estimated bite force, we suggest that *N. engaeus* was capable of crushing hard biological material such as bones. Based on our results, we conclude that the shape of the skull of *N. engaeus* allows a zoophagous diet, possibly hunting small living prey up to 20 kg (*e.g.*, young dicynodonts, cynodonts, little diapsids, prosauropods hatching specimens, eggs, and nestlings), and/or feeding on carcasses of big animals. Although the possibility of capturing a live prey does not only depend on the mechanical properties of the skull, this analysis allows us to get closer to the *N. engaeus* diet. Future biomechanical studies on the postcranium will allow us to better understand how *N. engaeus* captured its food. This new information, using a quantitative method, helps to understand the ecological role of the aetosaurs in Late Triassic communities.

ACKNOWLEDGMENTS

This work was part of the PhD thesis of J.R.A. Taborda, conducted in the Facultad de Ciencias Exactas y Naturales at the Universidad de Buenos Aires (Argentina) under the guidance of J.B. Desojo and E.N. Dvorkin. We thank to several people that helped to we make this paper: Jaime Powell☞ (PVL), Gabriela Cisterna (PULR), and Julian Faivovich (MACN-HE), who allowed us to study specimens under their care; Miguel Tauro for making the CTscan of the material at the Sagrada Familia Clinica. We are grateful for the comments and suggestions provided by several colleagues that helped to improve the present contribution, especially to Josep Fortuny, Sterling Nesbitt, and Claudia Tambussi. We thank two anonymous reviewers and the editor J. Wilson Mantilla for his comments on this manuscript. This research was partially funded by Agencia Nacional de Promoción Científica y Técnica (PICT 2014 Nº 609 and PICT 2018 Nº 0717 to JBD) and Consejo Nacional de Investigaciones Científicas y Tecnológicas (PUE 2016-CONICET- CICTERRA).

REFERENCES

Attard, M. R. G., Wilson, L. A. B., Worthy, T. H., Scofield, P., Johnston, P., Parr, W. C. H., & Wroe, S. (2016). Moa diet fits the bill: virtual reconstruction incorporating mummified remains and prediction of biomechanical performance in avian giants. *Proceedings of the Royal Society B Biological Sciences*, *283*, 20152043.

Bathe, K.-J. (1996). *Finite Element Procedures*. Prentice-Hall.

Bertin, T. J. C., Thivichon-Prince, B., LeBlanc, A. R. H., Caldwell, M. W., & Viriot, L. (2018). Current perspectives on tooth implantation, attachment, and replacement in amniota. *Frontiers in Physiology*, *9*(NOV), 1–20.

Biacchi Brust, A. C., Desojo, J. B., Schultz, C. L., Paes-Neto, V. D., Da-Rosa, Á. A. S., & Paes-neto, D. (2018). Osteology of the first skull of *Aetosauroides scagliai* Casamiquela 1960 (Archosauria: Aetosauria) from the Upper Triassic of Southern Brazil (*Hyperodapedon* Assemblage Zone) and its phylogenetic importance. *PLoS ONE*, 13(8), e0201450.

Bona, P., & Desojo, J. B. (2011). Osteology and cranial musculature of *Caiman latirostris* (crocodylia: Alligatoridae). *Journal of Morphology*, *272*(7), 780–795.

Bonaparte, J. F. (1969). Los tetrápodos triásicos de Argentina. *1º Internacional Symposium of Gondwana*, 307–325. Mar del Plata, 1967.

Bonaparte, J. F. (1971). Los tetrápodos del sector superior de la Formación Los Colorados, La Rioja, Argentina (Triásico Superior). Opera Lilloana XXII. In *Opera Lilloana XXII*. Tucumán: Fundación e Instituto Miguel Lillo.

Bonaparte, J. F. (1973). Edades reptil para Triasico de Argentina y Brasil. *V Congreso Geológico Argentino*, 93–129. Villa Carlos Paz, Cordoba: Asocoación Geológica Argentina.

448 Bonaparte, J. F. (1978). El Mesozoico de America del Sur y sus tetrapodos. Opera Lilloana
449 26. In *Opera Lilloana 26*. Tucumán: Ministerio de Cultura y Educación; Fundación
450 Miguel Lillo.
451 Borelli, A. G. (1680). *De motu animalium. Opus posthumum: pars prima*. ex typographia
452 Angeli Bernabò.
453 Button, D. J., Barrett, P. M., Rayfield, E. J., & Benson, R. (2016). Comparative cranial
454 myology and biomechanics of *Plateosaurus* and *Camarasaurus* and evolution of the
455 sauropod feeding apparatus. *Palaeontology*, *59*(6), 887–913.
456 Button, D. J., Rayfield, E. J., & Barrett, P. M. (2014). Cranial biomechanics underpins high
457 sauropod diversity in resource-poor environments. *Proceedings of the Royal Society B*,
458 *281*, 20142114.
459 Casamiquela, R. M. (1961). Dos nuevos estagonolepoideos Argentinos (de Ischigualasto,
460 San Juan). *Revista de La Asociación Geológica Argentina*, *16*, 143–203.
461 Case, E. C. (1920). Preliminary description of new suboder of puytosaurian reptiles with a
462 description of new species of *Phytosaurus*. *Journal of Geology*, *28*, 524–535.
463 Cerda, I. A., & Desojo, J. B. (2011). Dermal armour histology of aetosaurs (Archosauria:
464 Pseudosuchia), from the Upper Triassic of Argentina and Brazil. *Lethaia*, *44*(4), 417–
465 428.
466 Cox, P. G., Rinderknecht, A., & Blanco, R. E. (2015). Predicting bite force and cranial
467 biomechanics in the largest fossil rodent using finite element analysis. *Journal of*
468 *Anatomy*, *226*(3), 215–223.
469 Curtis, N., Jones, M. E. H., Shi, J., O'Higgins, P., Evans, S. E., & Fagan, M. J. (2011).
470 Functional relationship between skull form and feeding mechanics in *Sphenodon*, and
471 implications for diapsid skull development. *PLoS ONE*, *6*(12), 31–33.

Daudin, F. M. (1802). *Histoire naturelle, générale et particulière, des reptiles* (Vol. 2). Paris: De l'Imprimerie de F. Dufart.

Degrange, F. J., Tambussi, C. P., Moreno, K., Witmer, L. M., & Wroe, S. (2010). Mechanical analysis of feeding behavior in the extinct "terror bird" *Andalgalornis steulleti* (Gruiformes: Phorusrhacidae). *PloS One*, *5*(8), e11856.

Desojo, J. B. (2003). Redescripción del aetosaurio *Chilenosuchus forttae* Casamiquela (Diapsida: Arcosauria): presencia de Triásico continental en el norte de Chile. *Revista Geológica de Chile*, *30*(1), 53–63.

Desojo, J. B., & Báez, A. M. (2005). El esqueleto postcraneano de *Neoaetosauroides* (Archosauria: Aetosauria) del Triásico Superior del centro-oeste de Argentina. *Ameghiniana*, *42*(1), 115–126.

Desojo, J. B., & Báez, A. M. (2007). Cranial morphology of the Late Triassic South American archosaur *Neoaetosauroides engaeus*: evidence for aetosaurian diversity. *Palaeontology*, *50*(1), 267–276.

Desojo, J. B., & Ezcurra, M. D. (2011). A reappraisal of the taxonomic status of *Aetosauroides* (Archosauria, Aetosauria) specimens from the Late Triassic of South America and their proposed synonymy with *Stagonolepis*. *Journal of Vertebrate Paleontology*, *31*(3), 596–609.

Desojo, J. B., Ezcurra, M. D., & Kischlat, E. E. (2012). A new aetosaur genus (Archosauria : Pseudosuchia) from the early Late Triassic of southern Brazil. *Zootaxa*, *3166*, 1–33.

Desojo, J. B., Heckert, A. B., Martz, J. W., Parker, W. G., Schoch, R. R., Small, B. J., & Sulej, T. (2013). Aetosauria: a clade of armoured pseudosuchians from the Upper Triassic continental beds. In S. J. Nesbitt, J. B. Desojo, & R. B. Irmis (Eds.), *Anatomy*,

Phylogeny and Palaeobiology of Early Archosaurs and their Kin (pp. 203–239). Geological Society.

Desojo, J. B., & Vizcaíno, S. F. (2009). Jaw biomechanics in the South American aetosaur *Neoaetosauroides engaeus*. *Paläontologische Zeitschrift*, *83*(4), 499–510.

Dróżdż, D. (2018). Osteology of a forelimb of an aetosaur *Stagonolepis olenkae* (Archosauria: Pseudosuchia: Aetosauria) from the Krasiejów locality in Poland and its probable adaptations for a scratch-digging behavior. *PeerJ*, *6*, e5595.

Dynowski, J. F., Nebelsick, J. H., Klein, A., & Roth-Nebelsick, A. (2016). Computational fluid dynamics analysis of the fossil crinoid *Encrinus liliiformis* (Echinodermata: Crinoidea). *PLoS ONE*, *11*(5), e0156408.

Erickson, G. M., Gignac, P. M., Steppan, S. J., Lappin, a. K., Vliet, K. a., Brueggen, J. D., Inouye, B.D., Kledzik, D. & Webb, G. J. W. (2012). Insights into the ecology and evolutionary success of crocodilians revealed through bite-force and tooth-pressure experimentation. *PLoS ONE*, *7*(3), e31781.

Fedorov, A., Beichel, R., Kalpathy-Cramer, J., Finet, J., Fillion-Robin, J. C., Pujol, S., Bauer, C., Jennings, D., Fennessy, F., Sonka, M., Buatti, J., Aylward, S., Miller, J. V., Pieper, S. & Kikinis, R. (2012). 3D Slicer as an image computing platform for the Quantitative Imaging Network. *Magnetic Resonance Imaging*, *30*(9), 1323–1341.

Fortuny, J., Marcé-Nogué, J., Gil, L., & Galobart, À. (2012). Skull mechanics and the evolutionary patterns of the otic notch closure in capitosaurs (Amphibia: Temnospondyli). *Anatomical Record*, *295*(7), 1134–1146.

Fortuny, J., Marcé-Nogué, J., Steyer, J.-S., de Esteban-Trivigno, S., Mujal, E., & Gil, L. (2016). Comparative 3D analyses and palaeoecology of giant early amphibians (Temnospondyli: Stereospondyli). *Scientific Reports*, *6*, 30387.

Fraas, O. (1877). *Aetosaurus ferratus*, die gepanzerte Vogelechse aus dem Stubensandstein bei Stuttgart. *Jahreshefte Des Vereins Für Vaterländische Naturkunde in Württemberg*, *33*, 1–21.

Galton, P. M. (1985). Diet of prosauropod dinosaurs from the late Triassic and early Jurassic. *Lethaia*, *18*(2), 105–123.

Gonzalez, G. A. J. (1974). *Safety Factors: A Conceptual Review*. (Tesis Doctoral. M. Sc. Thesis-Imperial College, London).

Gregory, J. T. (1953). *Typothorax* scutes from Germany. *Postilla*, *15*, 1–6.

Gröning, F., Jones, M. E. H., Curtis, N., Herrel, A., O'Higgins, P., Evans, S. E., & Fagan, M. J. (2013). The importance of accurate muscle modelling for biomechanical analyses: a case study with a lizard skull. *Journal of the Royal Society, Interface / the Royal Society*, *10*(84), 20130216.

Halsey, L. G., & White, C. R. (2010). Measuring energetics and behaviour using accelerometry in cane toads *Bufo marinus*. *PLoS ONE*, *5*(4), e10170.

Heckert, A. B., & Lucas, S. G. (1999). A new aetosaur (Reptilia: Archosauria) from the Upper Triassic of Texas and the phylogeny of aetosaurs. *Jurnal of Vertebrate Paleontology*, *19*(1), 50–68.

Heckert, A. B., & Lucas, S. G. (2000). Taxonomy, phylogeny, biostratigraphy, biochronology, paleobiogeography, and evolution of the Late Triassic Aetosauria. *Zentralbalt Für Geologie Und Paläotologie, Teil I*(Heft 11-12), 1539–1587.

Heckert, A. B., & Lucas, S. G. (2002). South American occurrences of the Adamanian (Late Triassic:Latest Carnian) index taxon *Stagonolepis* (Archosauria: Aetosauria) and their biochronological significance. *Journal of Paleontology*, *76*(5), 852–863.

Heckert, A. B., Lucas, S. G., Rinehart, L. F., Celeskey, M. D., Spielmann, J. a., & Hunt, A.

544 P. (2010). Articulated skeletons of the aetosaur *Typothorax coccinarum* Cope
545 (Archosauria: Stagonolepididae) from the Upper Triassic Bull Canyon Formation
546 (Revueltian: early-mid Norian), eastern New Mexico, USA. *Journal of Vertebrate*
547 *Paleontology*, *30*(3), 619–642.
548 Holliday, C. M., Tsai, H. P., Skiljan, R. J., George, I. D., & Pathan, S. (2013). A 3D
549 Interactive Model and Atlas of the Jaw Musculature of *Alligator mississippiensis*.
550 *PLoS ONE*, *8*(6), e62806.
551 Holliday, C. M., & Witmer, L. M. (2007). Archosaur adductor chamber evolution:
552 Integration of musculoskeletal and topological criteria in jaw muscle homology.
553 *Journal of Morphology*, *268*(6), 457–484.
554 Iordansky, N. (2000). Jaw muscles of the crocodiles: structure, synonymy, and some
555 implications on homology and functions. *Russian Journal of Herpetology*, 7(1), 41–
556 50.
557 Jones, M. E. H., Curtis, N., O'Higgins, P., Fagan, M., & Evans, S. E. (2009). The head and
558 neck muscles associated with feeding in *Sphenodon* (Reptilia: Lepidosauria:
559 Rhynchocephalia). *Palaeontologia Electronica*, *12*(2), 7A:56p.
560 Kardong, K. V. (2011). *Vertebrates: Comparative Anatomy, Function, Evolution.* (6th ed.).
561 New York: McGraw-Hill.
562 Lautenschlager, S. (2016). Reconstructing the past: methods and techniques for the digital
563 restoration of fossils. *Royal Society Open Science*, *3*(10), 160342.
564 Lautenschlager, S. (2017). Functional niche partitioning in Therizinosauria provides new
565 insights into the evolution of theropod herbivory. *Palaeontology*, *60*(3), 375–387.
566 Lautenschlager, S., Witmer, L. M., Altangerel, P., & Rayfield, E. J. (2013). Edentulism,
567 beaks, and biomechanical innovations in the evolution of theropod dinosaurs.

Proceedings of the National Academy of Sciences, *110*(51), 20657–20662.

Lemanis, R., Zachow, S., & Hoffmann, R. (2016). Comparative cephalopod shell strength and the role of septum morphology on stress distribution. *PeerJ*, *4*, e2434. Retrieved from https://peerj.com/articles/2434

Long, R. A., & Ballet, K. L. (1985). Aetosaur dermal armor from the Late Triassic of southwestern North America, with special reference to material from the Chinle Formation of Petrified Forest National Park. *Museum of Northern Arizona Bulletin*, *47*, 45–68.

Marcé-Nogué, J., Fortuny, J., De Esteban-Trivigno, S., Sánchez, M., Gil, L., & Galobart, À. (2015). 3D Computational Mechanics Elucidate the Evolutionary Implications of Orbit Position and Size Diversity of Early Amphibians. *PLoS ONE*, *10*(6), e0131320.

McCurry, M. R., Mahony, M., Clausen, P. D., Quayle, M. R., Walmsley, C. W., Jessop, T. S., Wroe, S., Richards, H. & McHenry, C. R. (2015). The relationship between cranial structure, biomechanical performance and ecological diversity in varanoid lizards. *PLoS ONE*, *10*(6), e0130625.

Moreno, K., Wroe, S., Clausen, P., McHenry, C., D'Amore, D. C., Rayfield, E. J., & Cunningham, E. (2008). Cranial performance in the Komodo dragon (*Varanus komodoensis*) as revealed by high-resolution 3-D finite element analysis. *Journal of Anatomy*, *212*(6), 736–746.

Newtton, I. S. (1687). *Philosophiæ Naturalis Principia Mathematica*. Samuel Pepys, Reg. Soc. Præses.

Padian, K., Li, C., & Pchelnikova, J. (2010). The trackmaker of *Apatopus* (Late Triassic, North America): implications for the evolution of archosaur stance and gait. *Palaeontology*, *53*(1), 175–189.

592 Parker, W. G. (2005). A new species of the Late Triassic aetosaur *Desmatosuchus*
593 (Archosauria: Pseudosuchia). *Comptes Rendus Palevol*, *4*(4), 327–340.
594 Parker, W. G. (2007). Reassessment of the aetosaur '*Desmatosuchus' chamaensis* with a
595 reanalysis of the phylogeny of the Aetosauria (Archosauria: Pseudosuchia). *Journal of*
596 *Systematic Palaeontology*, *5*(1), 41–68.
597 Parker, W. G. (2008). Description of new material of the aetosaur *Desmatosuchus spurensis*
598 (Archosauria: Suchia) from the Chinle Formation of Arizona and a revision of the
599 genus *Desmatosuchus*. *PaleoBios*, *28*(1), 1–40.
600 Parker, W. G. (2016). Revised phylogenetic analysis of the Aetosauria (Archosauria:
601 Pseudosuchia); assessing the effects of incongruent morphological character sets.
602 *PeerJ*, *4*, e1583. Retrieved from https://peerj.com/articles/1583
603 Parker, W. G. (2018a). Anatomical notes and discussion of the first described aetosaur
604 *Stagonolepis robertsoni* (Archosauria: Suchia) from the Upper Triassic of Europe, and
605 the use of plesiomorphies in aetosaur biochronology. *PeerJ*, *6*, e5455.
606 Parker, W. G. (2018b). Redescription of *Calyptosuchus* (*Stagonolepis*) *wellesi*
607 (Archosauria: Pseudosuchia: Aetosauria) from the Late Triassic of the Southwestern
608 United States with a discussion of genera in vertebrate paleontology. *PeerJ*, *6*, e4291.
609 Parrish, J. M. (1986). Locomotor adaptations in the hind limb and pelvis of the
610 Thecodontia. *Hunteria*, *1*, 3–35.
611 Parrish, J. M. (1994). Cranial osteology of *Longosuchus meadei* and the phylogeny and
612 distribution of the Aetosauria. *Journal of Vertebrate Paleontology*, *14*(2), 196–209.
613 Porro, L. B., Holliday, C. M., Anapol, F., Ontiveros, L. C., Ontiveros, L. T., & Ross, C. F.
614 (2011). Free body analysis, beam mechanics, and finite element modeling of the
615 mandible of *Alligator mississippiensis*. *Journal of Morphology*, *272*(8), 910–937.

Qasem, L., Cardew, A., Wilson, A., Griffiths, I., Halsey, L. G., Shepard, E. L. C., … Wilson, R. (2012). Tri-axial dynamic acceleration as a proxy for animal energy expenditure; should we be summing values or calculating the vector? *PLoS ONE*, *7*(2), e31187.

Rayfield, E. J. (2007). Finite element analysis and understanding the biomechanics and evolution of living and fossil organisms. *Annual Review of Earth and Planetary Sciences*, *35*(1), 541–576.

Reid, R. E. H. (1996). Bone histology of the Cleveland-Lloyd dinosaurs and of dinosaurs in general, Part I: Introduction: Introduction to bone tissues. *Brigham Young University Geology Studies*, *41*, 25–72.

Richmond, B. G., Wright, B. W., Grosse, I., Dechow, P. C., Ross, C. F., Spencer, M. a, & Strait, D. S. (2005). Finite element analysis in functional morphology. *The Anatomical Record. Part A, Discoveries in Molecular, Cellular, and Evolutionary Biology*, *283*(2), 259–274.

Ross, C. F. (2005). Finite element analysis in vertebrate biomechanics. *The Anatomical Record. Part A, Discoveries in Molecular, Cellular, and Evolutionary Biology*, *283*(2), 253–258.

Ross, C. F., Patel, B. a, Slice, D. E., Strait, D. S., Dechow, P. C., Richmond, B. G., & Spencer, M. a. (2005). Modeling masticatory muscle force in finite element analysis: sensitivity analysis using principal coordinates analysis. *The Anatomical Record. Part A, Discoveries in Molecular, Cellular, and Evolutionary Biology*, *283*(2), 288–299.

Sawin, H. J. (1947). The pseudosuchian reptile *Typothorax meadei* [Dockum Triassic, Texas]. *Journal of Paleontology*, *21*(3), 201–238.

Schoch, R. R. (2007). Osteology of the small archosaur *Aetosaurus* from the Upper Triassic

of Germany. *Neues Jahrbuch Für Geologie Und Paläontologie - Abhandlungen*, *246*(1), 1–35.

Schoch, R. R., & Desojo, J. B. (2016). Cranial anatomy of the aetosaur Pa*ratypothorax andressorum* Long & Ballew, 1985, from the Upper Triassic of Germany and its bearing on aetosaur phylogeny. *Neues Jahrbuch Für Geologie Und Paläontologie - Abhandlungen*, *279*(1), 73–95.

Schwager, H., Masselter, T., Speck, T., & Neinhuis, C. (2013). Functional morphology and biomechanics of branch-stem junctions in columnar cacti. *Proceedings of the Royal Society B*, *280*(1772), 20132244.

Sellers, K. C., Middleton, K. M., Davis, J. L., & Holliday, C. M. (2017). Ontogeny of bite force in a validated biomechanical model of the American alligator. *The Journal of Experimental Biology*, *220*(11), 2036–2046.

Small, B. J. (2002). Cranial anatomy of *Desmatosuchus haplocerus* (Reptilia: Archosauria: Stagonolepididae). *Zoological Journal of the Linnean Society*, *136*(1), 97–111.

Small, B. J., & Martz, J. W. (2013). A new aetosaur from the Upper Triassic Chinle Formation of the Eagle Basin, Colorado, USA. In S. J. Nesbitt, J. B. Desojo, & R. B. Irmis (Eds.), *Anatomy, Phylogeny and Palaeobiology of Early Archosaurs and Their Kin* (pp. 393–412). Geological Society.

Snively, E., Fahlke, J. M., & Welsh, R. C. (2015). Bone-breaking bite force of *Basilosaurus isis* (Mammalia , Cetacea) from the late Eocene of Egypt estimated by Finite Element Analysis. *PLoS ONE*, *10*(2), 1–23.

Sulej, T. (2010). The skull of an early Late Triassic aetosaur and the evolution of the stagonolepidid archosaurian reptiles. *Zoological Journal of the Linnean Society*, *158*(4), 860–881.

Taborda, J. R. A. (2011). *Dinámica del crecimiento de Aetosauroides scagliai Casamiquela, 1960 (Archosauria : Aetosauria) del Triásico Tardío de América del Sur*. (Tesis de Licensiatura, Facultad de Ciencias Exactas y Naturales, Universidad de Buenos Aires, Buenos Aires).

Taborda, J. R. A. (2016). *Estructura y función cráneodentaria: un acercamiento a la paleobiología de los aetosaurios sudamericanos (Archosauria: Pseudosuchia).* (Tesis Doctoral, Facultad de Ciencias Exactas y Naturales, Universidad de Buenos Aires, Buenos Aires).

Taborda, J. R. A., Cerda, I. A., & Desojo, J. B. (2013). Growth curve of *Aetosauroides scagliai* Casamiquela 1960 (Pseudosuchia: Aetosauria) inferred from osteoderm histology. In S. J. Nesbitt, J. B. Desojo, & R. B. Irmis (Eds.), *Anatomy, Phylogeny and Palaeobiology of Early Archosaurs and Their Kin* (pp. 413–423). Geological Society.

Taborda, J. R. A., & Desojo, J. B. (2010). Revisión de la morfología dentaria del aetosaurio *Neoaetosauroides engaeus*: nuevos datos e implicancias. *Ameghiniana, 47*(4), 19R.

Taborda, J. R. A., & Desojo, J. B. (2015). Análisis biomecánico craneano del aetosaurio *Neoaetosauroides engaeus* Bonaparte 1969 (Archosauria: Pseudosuchia) utilizando el Método de los Elementos Finitos. *Ameghiniana, 52*(4), 37R. Diamante.

Tsai, H. P., & Holliday, C. M. (2011). Ontogeny of the *Alligator* cartilago *transiliens* and its significance for sauropsid jaw muscle evolution. *PLoS ONE, 6*(9), e24935.

von Baczko, M. B., Taborda, J. R. A., & Desojo, J. B. (2018). Paleoneuroanatomy of the aetosaur *Neoaetosauroides engaeus* (Archosauria: Pseudosuchia) and its paleobiological implications among archosauriforms. *PeerJ, 6*, e5456.

Walker, A. D. (1961). Triassic reptiles from the Elgin area: *Stagonolepis, Dasygnathus* and their allies. *Philosophical Transactions of the Royal Society of London. Series B,*

688 *Biological Sciences*, *244*(709), 103–204.
689 Wroe, S., Chamoli, U., Parr, W. C. H., Clausen, P., Ridgely, R., & Witmer, L. M. (2013).
690 Comparative biomechanical modeling of metatherian and placental saber-tooths: a
691 different kind of bite for an extreme pouched predator. *PLoS ONE*, *8*(6), 8–16.
692 Wroe, S., Huber, D. R., Lowry, M., McHenry, C., Moreno, K., Clausen, P., Ferrara, T.L.,
693 Cunningham, E., Dean, M. N. & Summers, A. P. (2008). Three-dimensional computer
694 analysis of white shark jaw mechanics: How hard can a great white bite? *Journal of*
695 *Zoology*, *276*(4), 336–342.
696 Wroe, S., Moreno, K., Clausen, P., Mchenry, C., & Curnoe, D. (2007). High-resolution
697 three-dimensional computer simulation of hominid cranial mechanics. *Anatomical*
698 *Record*, *290*(10), 1248–1255.
699 Young, M.T., Rayfield, E.J., Holliday, C.M., Witmer, L.M., Button, D.J., Upchurch, P. &
700 Barrett, P.M. 2012. Cranial biomechanics of *Diplodocus* (Dinosauria, Sauropoda):
701 Testing hypotheses of feeding behaviour in an extinct megaherbivore.
702 *Naturwissenschaften* 99(8): 637–643. DOI:10.1007/s00114-012-0944-y.
703 Zapata, U., Metzger, K., Wang, Q., Elsey, R. M., Ross, C. F., & Dechow, P. C. (2010).
704 Material properties of mandibular cortical bone in the American alligator, *Alligator*
705 *mississippiensis*. *Bone*, *46*(3), 860–867.
706 Zienkiewicz, O. C., & Taylor, R. L. (1994a). *El Metodo de los Elementos Finitos. Volumen*
707 *1: Formulación básica y problemas lineales* (4th ed.). McGraw-Hill.
708 Zienkiewicz, O. C., & Taylor, R. L. (1994b). *El Metodo de los Elementos Finitos. Volumen*
709 *2: Macánica de Sólidos y Fluidos. Dinámica y no linealidad* (4th ed.). McGraw-Hill.

Figure captions

Figure 1. Models of three referred cranial specimens merged to make the complete 3D model of skull for ***Neoaetosauroides engaeus***. We combined the 3D model obtained by segmentation from CT-scan of specimens **PVL5698** (**1**), **PVL4363** (**2**) and **PULR108** (**3**), to make the structure of complete skull (**4**). The 3D views are available in supplementary materials. Scale bar equals 2 cm

Figure 2. 1-3, Tooth morphology of ***Neoaetosauroides engaeus*** specimen **PULR108**. **4-5,** Comparison with similar tooth morphology observed in other aetosaurs and in living crocodiles. **1,** Cast of pramaxillary teeth; **2,** Labial cast of right maxilla with teeth and part of the mandible; **3,** Detail of the best preserved tooth and its 3D reconstruction: **4,** Posterior and middle tooth from maxilla ***Caiman yacare*** (**MACN-HE 43694**); **5,** Tooth from the maxilla of ***Stagonolepis olenkae*** (**ZPAL AbIII/1995**). Scale bar equals 1 cm.

Figure 3. 3D reconstruction of adductor chamber musculature for ***Neoaetosauroides engaeus***. Abbreviations: **mAMP**: *musculus adductor mandibulae posterior*, **mAMEs/m/p**: *musculus adductor mandibulae externus superficialis* / *medialis* / *profundus*, **mPST**: *musculus pseudotemporalis*, **mIM**: *musculus intramandibularis*, **mPTv/d** *musculus pterygoideus ventralis*/*dorsalis*.

Figure 4. Modeling *musculus adductor mandibulae posterior*: **1,** Volume 3D representation; **2,** Muscles modeled using muscular action bars; **3,** Mesh of the finite

element model indicating the points for each analysis of Bite force and external load force in ***Neoaetosauroides engaeus***.

Figure 5. Result of FEA for bite force test, bilateral (**top**), unilateral (**bottom**) and mandible tip (**middle**). The bite force was measured among points **A**, **C** and **D** (see Fig 4). The colorimetric scale shows the effective (von Mises) stress distribution in the structure. Scale bar equals 5 cm.

Figure 6. Result of FEA for external load force, tractive (**top**) and lateral (**bottom**), during the bite. The bilateral external force was applied among the points **A**, **B** and **C** (see Fig 4). The colorimetric scale shows the effective (von Mises) stress distribution in the structure. Scale bar equals 5 cm

Figure 7. Result of FEA for a vertical external force emplaced at the lateral expansion of premaxilla of ***Neoaetosauroides engaeus***. **1,** right lateral view; **2**, ventral view. The colorimetric scale shows the effective (von Mises) stress distribution in the structure, and the maximums value corresponds to the shear modulus of bone. Scale bar equals 5 cm.

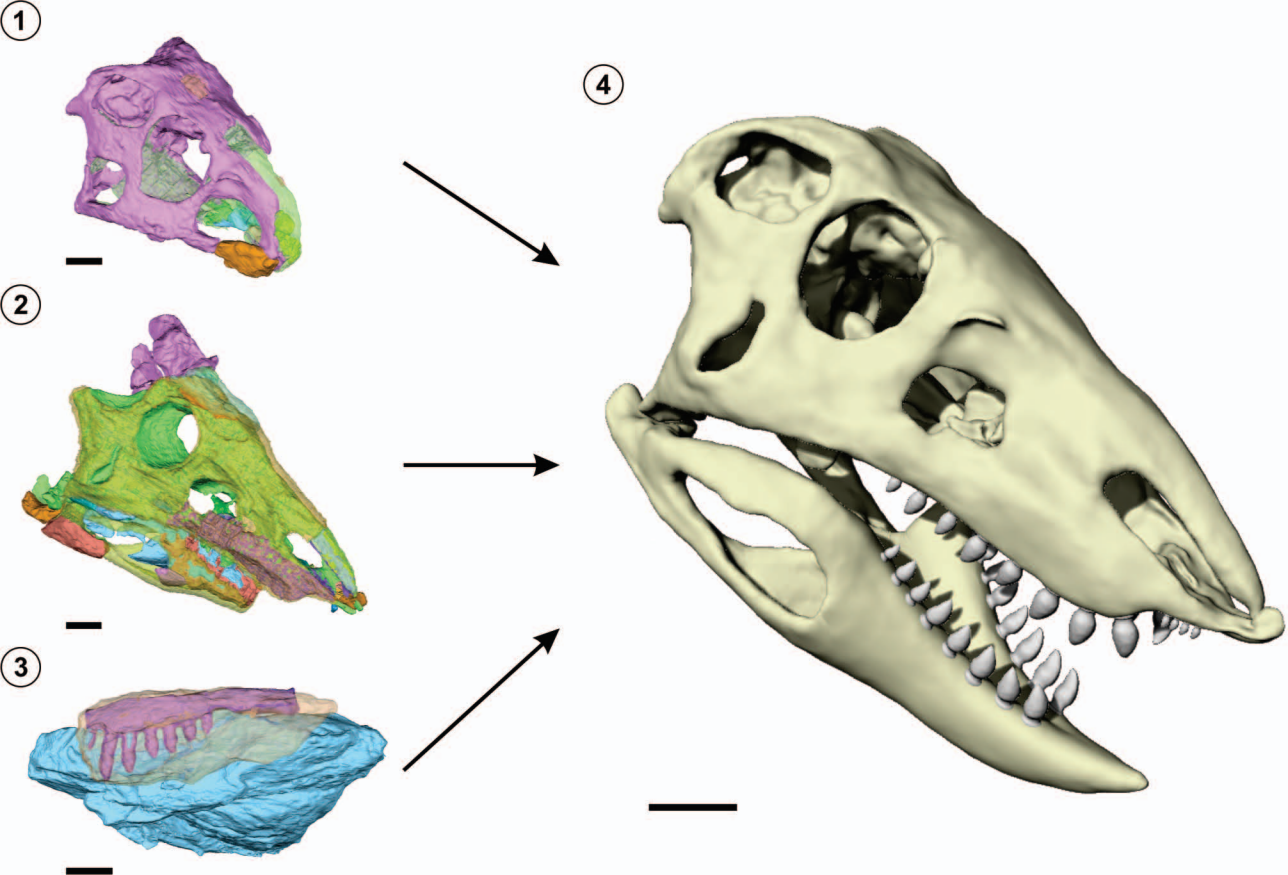
1
2
3
4

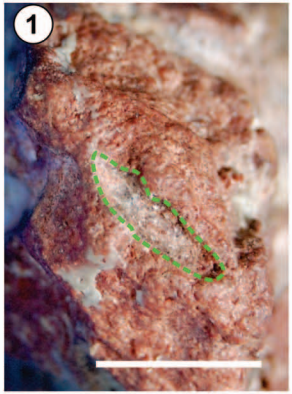
1

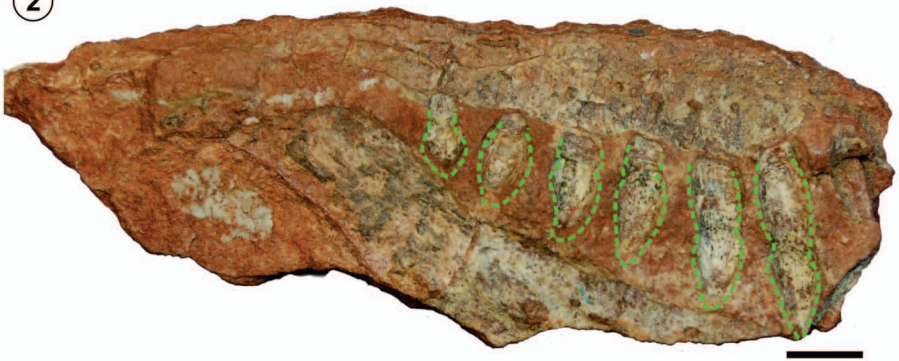
2

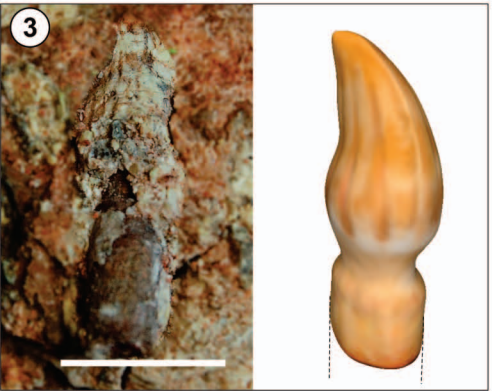
3


4


5

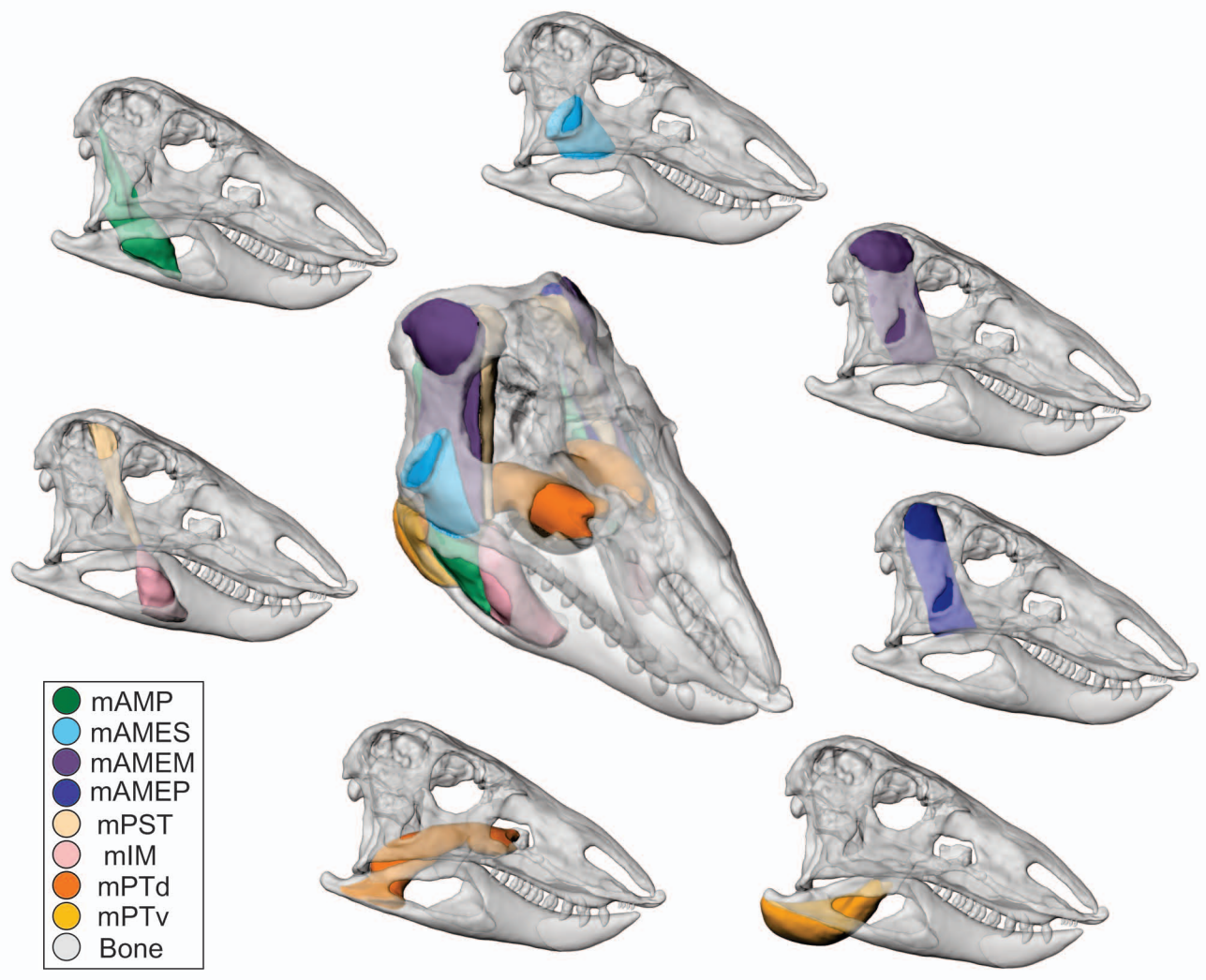
mAMP
mAMES
mAMEM
mAMEP
mPST
mIM
mPTd
mPTv
Bone

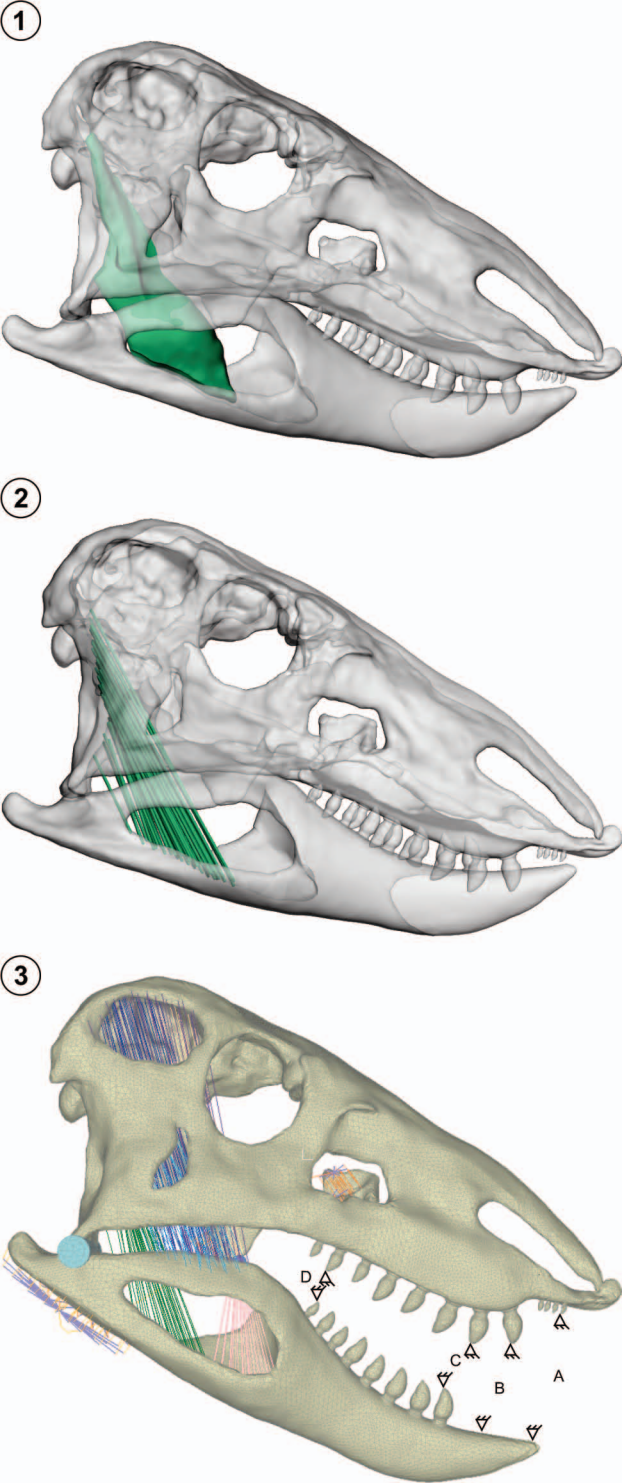
1
2
3
D
C
B
A

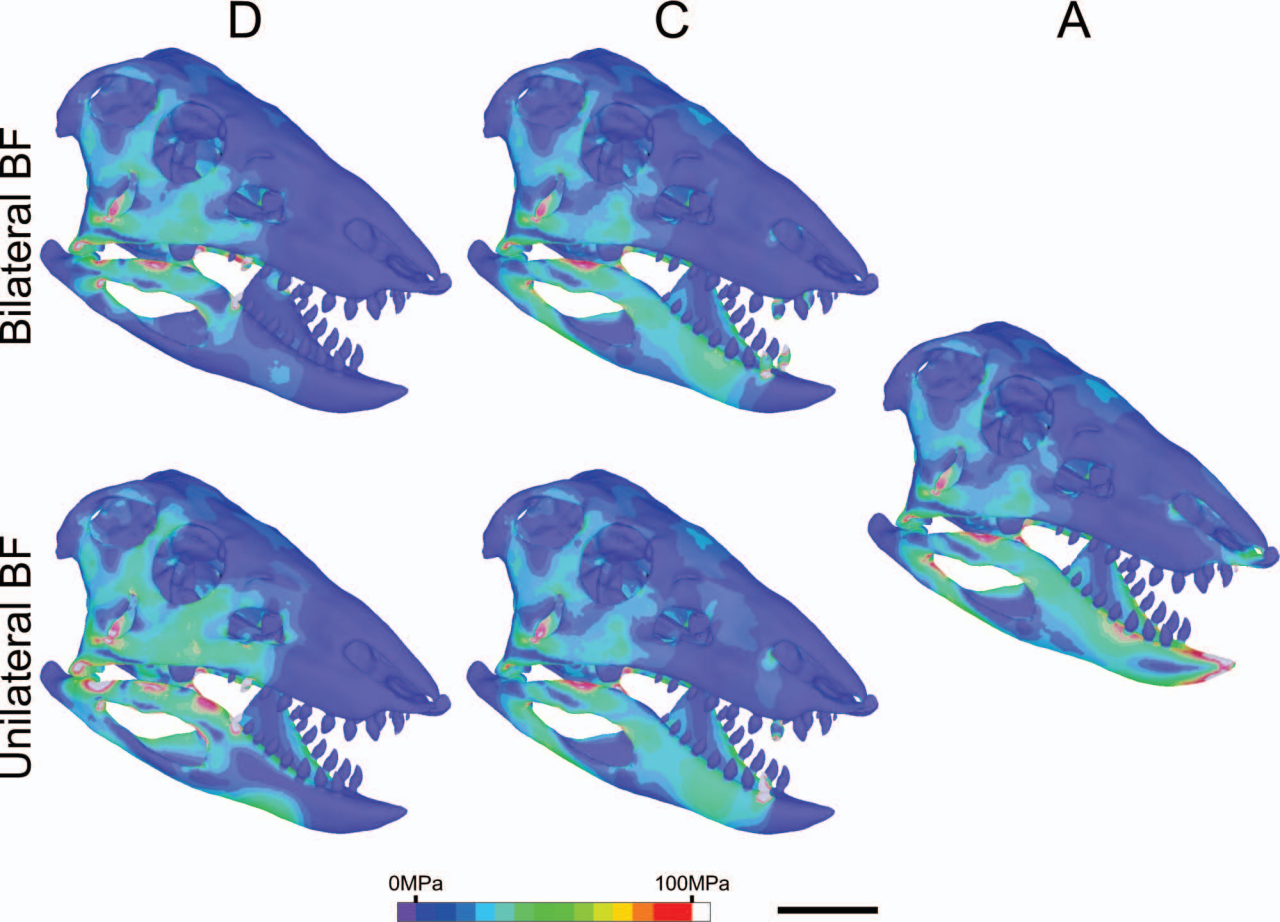
D
C
A
Bilateral BF
Unilateral BF
0MPa
100MPa

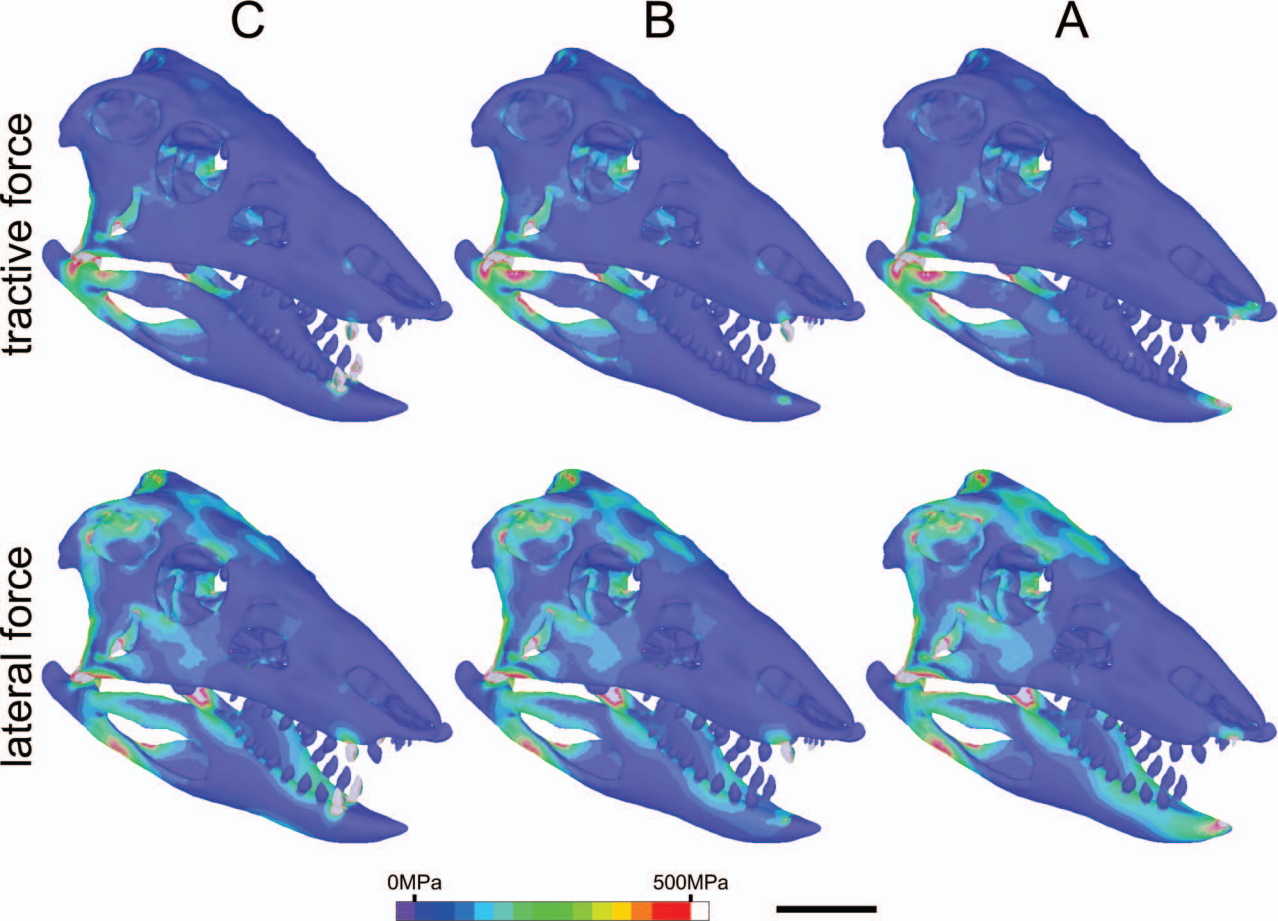
C
B
A
tractive force
lateral force
0MPa
500MPa

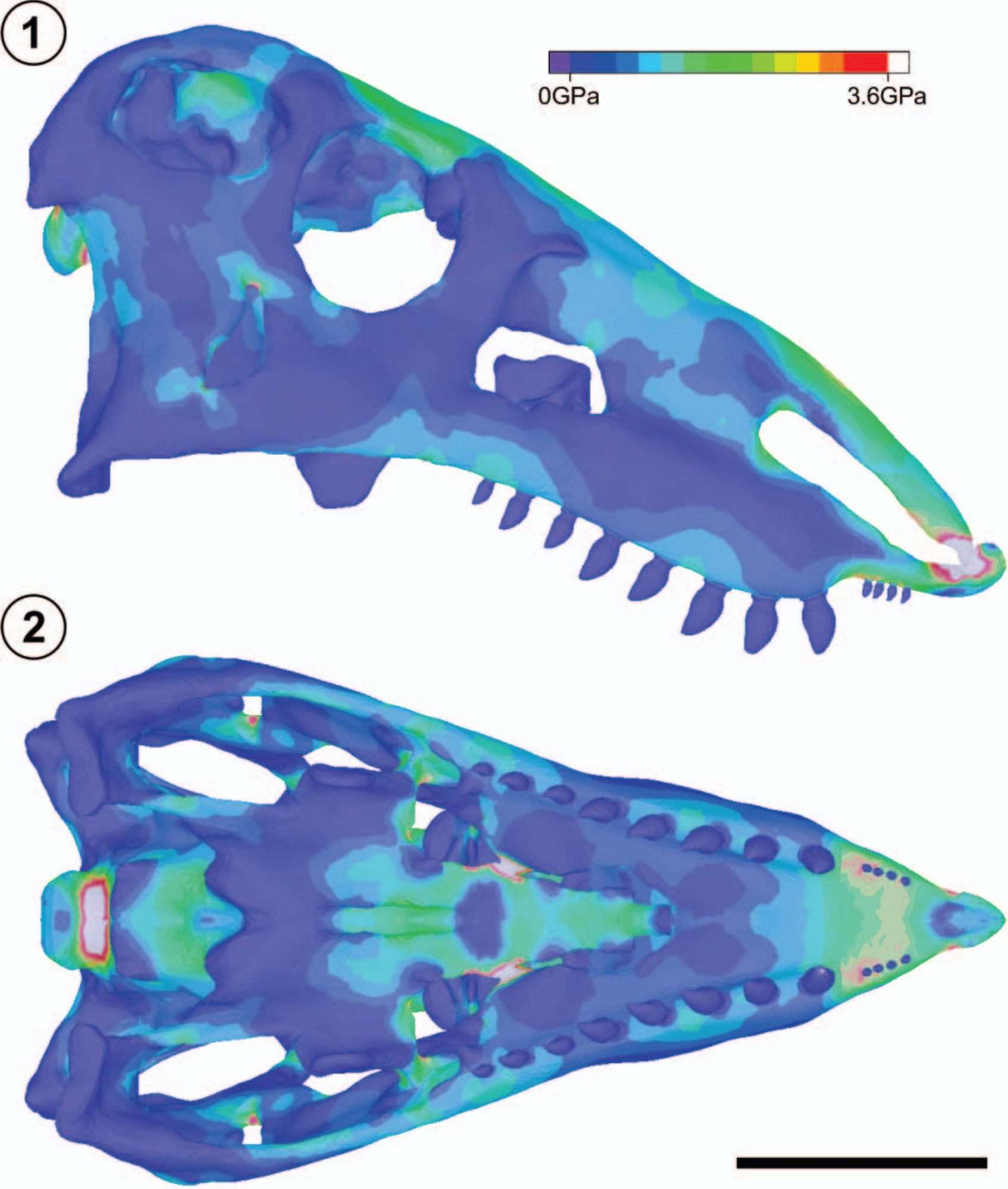
1
0GPa
3.6GPa
2

TABLE 1: Specifications of DICOM series for each specimen of *N. engaeus* tomographed.

Specimen	#slices	ST [mm]	IS [mm]	FOV [mm]	Power [KV]	I-Xray [mA]	ExpT [mseg]	Expoure
PULR 108	336	0.625	5	188	140	200	1117	10
PVL 4363	402	0.8	0.4	336	120	305	657	200
PVL 5698	413	0.9	0.45	289	120	313	640	200

Slices = number of slices. ExpT= exposure time. FOV= field of view. IS= ienter-slice. I-Xray= Xray tube current. ST= slice thickness

TABLE 2. Values for the modelization of the adductor chamber muscles force.

Muscle	PCSA [mm^2]	F [N]
mAMP	345.34	86.33
mAMEs	559.55	139.89
mAMEm	217.29	54.32
mAMEp	156.79	39.20
mPsT	338.52	84.63
mIM	280.30	70.07
mPTd	432.72	108.18
mPTv	807.62	201.90

F = estimated muscles. PCSA= estimated physiological cross-sectional area.

TABLE 3. Material properties.

Tissue	ε [GPa]	ν
bone	15	3.9
cranio-mandibular articulation	0.1	0.4
transiliens cartilage	1	0.4

ε = Young's modulus. ν = Poisson's ratio

TABLE 4. Measured bite force with FEA in different point of jaw.

Point	Fu [N]	Fb [N]
A	-	3000.9
C	3610	3764.7
D	5548	5810

Fb = bilateral bite force. Fu = unilateral bite force.